Electrochemical properties of a Si thin-film anode deposited on a TiNi shape-memory-alloy thin film

Joo-Hyeon Bae[1] · Nyamaa Oyunbayar[2] · Duck-Hyeon Seo[3] · Jeong-Hyeon Yang[4] · Tae-Hyun Nam[5]

Sun-Chul Huh[6] · Hyo-Min Jeong[7] · Jung-Pil Noh[†]

Abstract: Advances in electronics have generated an increasing demand for smaller, higher-capacity lithium-ion batteries, which will require alternatives to graphite as the battery anode material. To this end, a TiNi shape-memory-alloy (SMA) thin film was fabricated on Cu foil by DC magnetron sputtering. Si thin films were then deposited at a low temperature (LT) of 298 K (Si(LT)/TiNi/Cu) and a high temperature (HT) of 853 K (Si(HT)/TiNI/Cu). The Si thin films formed were amorphous regardless of the deposition temperature. The grain sizes of Si deposited at 298 K and 853 K were measured as 261 nm and 187 nm, respectively. The Si(HT)/TiNi/Cu electrode exhibited excellent capacity retention until approximately the 45th cycle, whereas rapid capacity fading occurred in the Si(LT)/TiNi/Cu electrode at the same current density of 200 μA/cm². The better cycle performance is attributed to increased adhesion force between the Si film and the TiNi SMA thin film because the stress generated in the Si thin film during the charge and discharge process was transferred to the TiNi SMA thin film, resulting in a stress absorption effect.

Keywords: TiNi shape-memory alloy, Thin films, Si anode, Stress absorption effect

1. Introduction

The development of the Internet of Things (IoT) and fifth-generation (5G) mobile communication requires flexible batteries with smaller sizes and larger capacities. To satisfy these demands, a number of studies have been conducted to achieve higher-capacity lithium-ion batteries using graphite anodes. However, the theoretical maximum capacity of commercial graphite electrodes has been reached (372 mAh/g) [1]. Therefore, to increase the capacity of lithium-ion batteries, the development of a new type of anode that replaces graphite is required.

Many anode active materials (Si, Sn, Ge, Al, etc.) have been studied as substitutes for graphite anodes. These materials have high volumetric and gravimetric capacities owing to their high lithium packing densities and safe thermodynamic potentials compared to carbonaceous materials [2]. In particular, silicon provides ten times the specific capacity (4200 mAh/g) of graphite [3]-[6]. However, large stresses because of dramatic volume changes in the processes of lithiation and delithiation can cause electrical contact loss between the active material and the current collector, which reduces the lifetime of the battery [7][8]. Therefore, many investigations have made progress in reducing

---

† Corresponding Author (ORCID: http://orcid.org/0000-0002-6937-2780): Professor, Department of Energy & Mechanical Engineering & Institute of Marine Industry, Gyeongsang National University, 2-13 Tongyeonghaean-daero, Tongyeong 53064, Republic of Korea, E-mail: nohjp@gnu.ac.kr, Tel: 055-772-9117

1 M. S., Department of Energy & Mechanical Engineering & Institute of Marine Industry, Gyeongsang National University, E-mail: jhyeonb@gnu.ac.kr, Tel: 055-772-9110

2 M. S., Department of Energy & Mechanical Engineering & Institute of Marine Industry, Gyeongsang National University, E-mail: n.oyuka1231@yahoo.com, Tel: 055-772-9110

3 M. S., Department of Energy & Mechanical Engineering & Institute of Marine Industry, Gyeongsang National University, E-mail: dudug17@gnu.ac.kr, Tel: 055-772-9110

4 Professor, Department of Mechanical System Engineering, Gyeongsang National University, E-mail: jh.yagi@gnu.ac.kr, Tel: 055-772-9107

5 Professor, Department of Materials Engineering and Convergence Technology & Research Institute for Green Energy Convergence Technology, Gyeongsang National University, E-mail: tahynam@gnu.ac.kr, Tel: 055-772-1665

6 Professor, Department of Energy & Mechanical Engineering & Institute of Marine Industry, Gyeongsang National University, E-mail: schuh@gnu.ac.kr, Tel: 055-772-9111

7 Professor, Department of Energy & Mechanical Engineering & Institute of Marine Industry, Gyeongsang National University, E-mail: hmjeong@gnu.ac.kr, Tel: 055-772-9114

Joo-Hyeon Bae ・ Nyamaa Oyunbayar ・ Duck-Hyeon Seo ・ Jeong-Hyeon Yang ・ Tae-Hyun Nam ・ Sun-Chul Huh ・ Hyo-Min Jeong ・ Jung-Pil Noh

this volume change. Mi-Hee Park *et al.* attempted to reduce the volume change by inserting silicon into nanotubes [9]. Li-Feing Cui *et al.* manufactured carbon-silicon core–shell nanowires, which reduced structural stress and damage during lithium cycling [10]. Shanshan Yin *et al.* demonstrated improved electrode structure stability and cyclic performance via a Si/Ag nanocomposite [11].

We reported that the volume change of the Si electrode could be reduced by using a TiNi shape-memory alloy (SMA) as a current collector [12][13]. This is because the stress generated during the volume change is absorbed throughout the TiNi SMA substrate. However, the TiNi current collector has a high thickness, and thus cannot be applied directly to a flexible battery.

In this study, we investigated the stress absorption effect of a TiNi SMA thin-film substrate. TiNi SMA and Si thin films were deposited by DC magnetron sputtering. The crystal structure was analyzed by X-ray diffraction (XRD), and the electrochemical properties were observed through cyclic voltammetry at constant curtain charge/discharge.

2. Experimental procedure

Si/TiNi thin films were fabricated on Cu foil by a DC magnetron sputtering system with pure Ti (99.9%), Ni (99.9%), and Si (99.99%) targets. The Cu foil was physically wiped with acetone and alcohol before deposition of the thin film. First, Ti and Ni were deposited under the following conditions: substrate temperature 853 K, Ar gas flow rate 20 sccm, substrate–target distance 80 mm, initial pressure 1.33×10^{-4} Pa, working pressure 0.27 Pa, and deposition time 120 min. The DC powers of the Ti and Ni targets were 180 W and 60 W, respectively. The composition of the prepared TiNi thin film was 50.3% Ti and 49.7 % Ni, as measured by energy-dispersive spectroscopy. The Si was then deposited on the TiNi layer with 200 W DC power for 30 min at 298 K or 853 K. (Here, the former at low temperature (LT) is named Si(LT)/TiNi/Cu, and the latter at high temperature (HT) is named Si (HT)/TiNi/Cu.) The other deposition conditions of the Si thin film were the same as those for the TiNi thin film. **Figure 1** shows a cross-section of the Si/TiNi thin film deposited on a glass substrate under the same growth conditions. The growth rates of TiNi and Si were 23.2 and 26.7 nm/min, respectively.

The composition, cross-section, and surface morphology of the deposited films were characterized using a field-emission scanning electron microscope equipped with an energy-dispersive X-ray spectrometer at 15 kV. The crystalline structure was characterized using an X-ray diffractometer with Cu K_α radiation (λ = 1.5418Å). Scans were performed over a 2θ range of 30–60º ° at a speed of 0.07º/s.

CR2032-type coin cells were fabricated with Si(LT)/TiNi/Cu and Si (HT)/TiNi/Cu cut into 10 mm diameter discs. The counter electrode and electrolyte were lithium foil and 1 M $LiPF_6$ in EC/DEC (1:1), respectively. Cyclic voltammetry was performed at a scanning rate of 0.1 mV/s in the voltage range 0.01–3.0 V. Constant current charge/discharge was performed at 200 $\mu A/cm^2$ corresponding to a 0.4 C rate and cut-off voltage was controlled between 0.01 V and 1.5 V.
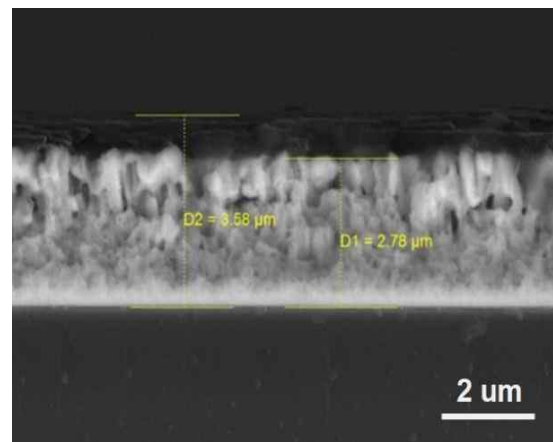

Figure 1: Cross-section of Si/TiNi thin film deposited on a glass substrate under the same growth conditions

3. Results and discussion

Figure 2 shows the surface morphology of the samples at each step. The surface of the Cu foil used as the current collector substrate is shown in **Figure 2 (a)**. The scratches seen on the surface were likely caused by physical wiping. This would increase the surface roughness and improve the adhesion of the subsequently deposited TiNi film. The surface morphology of the TiNi film deposited on the Cu foil is shown in **Figure 2 (b)**. Rough features such as cube corners appear on the deposited TiNi surface. The grain size of the TiNi film calculated from the surface is approximately 189 nm. **Figures 2 (c)** and **(d)** represent the surface morphology of Si deposited at 298 K and 853 K, respectively. As shown in **Figures 2 (c)** and **(d)**, the surface cluster morphology is similar regardless of the deposition temperature. The grain sizes were calculated as 261 nm and 187 nm at 298 K and 853 K, respectively.
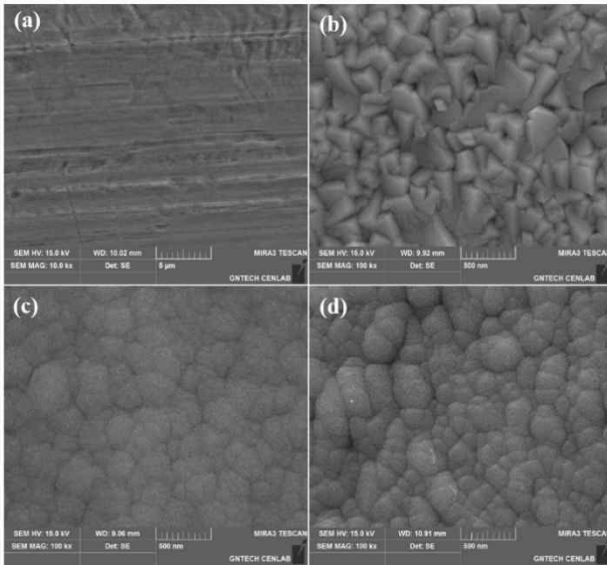
Figure 2: Surface morphologies of the samples of (a) Cu surface, (b) TiNi/Cu, (c) Si(LT)/TiNi/Cu, and (d) Si(HT)/TiNi/Cu

The crystal structures of the deposited thin films were investigated by XRD analysis and are shown in **Figure 3**. **Figures 3 (a)** and **(b)** show the XRD patterns of the Cu foil and the deposited TiNi layer on the Cu foil. As seen in **Figure 3 (b)**, rhombohedral-phase (R-phase) peaks can be observed at 42.4° and 42.8°. **Figures 3 (c)** and **(d)** show the XRD patterns of Si(LT)/TiNi/Cu and Si (HT)/TiNi/Cu, respectively. No crystalline Si peak was observed in either sample. This means that the deposited Si layer is either amorphous or nanostructured. The R-phase of the TiNi film changed to a cubic phase (B2 phase). Lattice strain is considered to have been caused by the stress generated in the Si deposition process **[14]**.
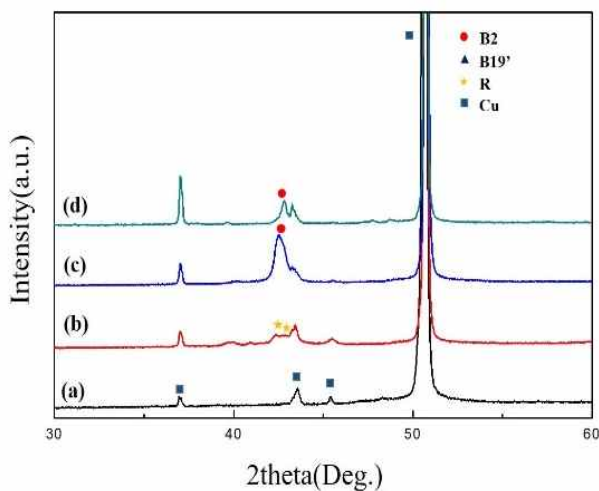

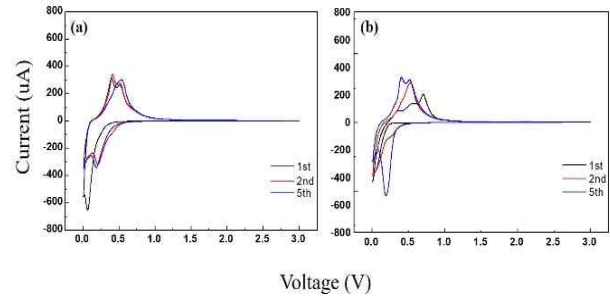**Figure 3:** XRD profiles of (a) Cu foil, (b) TiNi/Cu, (c) Si(LT)/TiNi/Cu, and (d) Si(HT)/TiNi/Cu

Figure 4: Cyclic voltammetry profiles (CV) of (a) Si(LT)/TiNi/Cu and (b) Si(HT)/TiNi/Cu electrodes

Figures 4 (a) and **(b)** show the typical cyclic voltammetry (CV) profiles of the Si(LT)/TiNi/Cu and Si(HT)/TiNi/Cu electrodes, respectively. In the first cathodic (lithiation) scan of the Si(LT)/TiNi/Cu electrode [**Figure 4 (a)**], the small and broad peak located at approximately 1.5 V (vs. Li/Li+) is attributed to the formation of a solid electrolyte interphase (SEI) film, which leads to irreversible capacity loss **[15]-[17]**. The peak centered at 0.34–0.02 V is attributed to the formation of a series of LixSi alloys. The peak close to 0.02 V can be attributed to the phase transition from LixSi to Li15Si4. After the second cathodic scan of the Si(LT)/TiNi/Cu electrode, the initial peaks decrease in intensity and shift in the higher-potential direction. For the anodic processes (delithiation), two broad peaks appear in the potential range of 0.26–0.61 V which originate from the delithiation reaction of Si. In the case of the first cathodic scan of the Si(HT)/TiNi/Cu electrode (**Figure 4 (b)**), the small and broad peaks located at approximately 1.6 V (vs. Li/Li+) are attributed to the formation of an SEI film. The peak located at 0.23 V to 0.01 V is narrower than that in the first cathodic scan of the Si(LT)/TiNi/Cu electrode. As the cycle repeats, the peak shifts to a higher voltage and becomes stronger. For the anodic processes, three broad peaks appear in the potential range 0.26–0.85 V, which originate from the delithiation reaction of Si. As the cycle repeats, the peaks shift to a lower voltage and become stronger and more stabilized.

Galvanostatic discharge/charge tests for the Si(LT)/TiNi/Cu and Si(HT)/TiNi/Cu electrodes were performed at a current density of 200 μA/cm^2 (**Figure 5**). As shown in **Figure 5 (a)**, the Si(LT)/TiNi/Cu electrode exhibits a discharging plateau at approximately 0.1 V after the initial potential drops rapidly to 0.2 V, and a small charging potential plateau at approximately 0.45 V in the first cycle. The initial rapid potential drop becomes noticeably gentler as the cycle repeats. The charge capacity of the Si(LT)/TiNi/Cu electrode after 30 cycles was 125

Joo-Hyeon Bae · Nyamaa Oyunbayar · Duck-Hyeon Seo · Jeong-Hyeon Yang · Tae-Hyun Nam · Sun-Chul Huh · Hyo-Min Jeong · Jung-Pil Noh

$\mu Ah/cm^2 \cdot \mu m$, which is approximately 24% of the capacity of the first cycle. For the Si(HT)/TiNi/Cu electrode (**Figure 5 (b)**), the main discharge/charge plateaus are very similar to those of the Si(LT)/TiNi/Cu electrode. However, during lithiation in the first cycle, there is a more severe initial potential drop (to 0.08 V). Similar to the Si(LT)/TiNi/Cu electrode, the initial rapid potential drop becomes noticeably gentler. The initial charge capacity gradually increases from 433 $\mu Ah/cm^2 \cdot \mu m$ to 570 $\mu Ah/cm^2 \cdot \mu m$ until the 10th cycle, and then stabilizes at the 35th cycle.
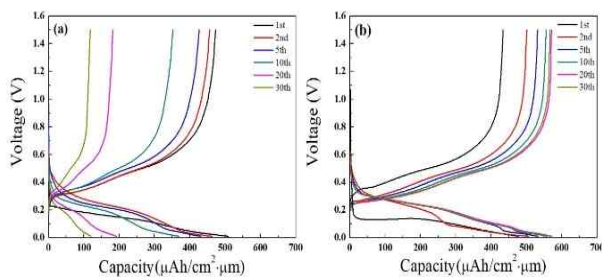

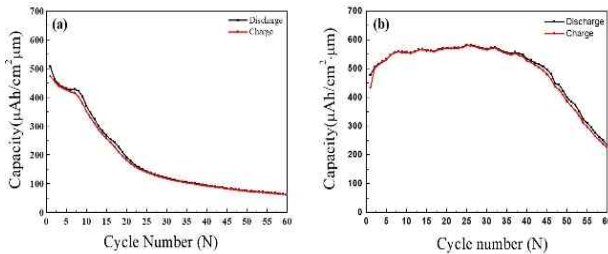**Figure 5:** Galvanostatic discharge/charge test for (a) Si(LT)/TiNi/Cu and (b) Si(HT)/TiNi/Cu electrodes

Figure 6: Cyclic performance of (a) Si(LT)/TiNi/Cu and (b) Si(HT)/TiNi/Cu electrodes

Figure 6 shows the cyclic performance of the Si(LT)/TiNi/Cu and Si(HT)/TiNi/Cu electrodes. As shown in **Figure 6 (a)**, the Si(LT)/TiNi/Cu electrode shows capacity retention (~415 $\mu Ah/cm^2 \cdot \mu m$) until the 7th cycle, but the capacity rapidly decreases to 117 $\mu Ah/cm^2 \cdot \mu m$ after the 30th cycle. In contrast, the charge capacity of the Si(HT)/TiNi/Cu electrode is stabilized at 570 $\mu Ah/cm^2 \cdot \mu m$ until the 45th cycle, as can be seen in **Figure 6 (b)**. It is considered that this difference is determined by whether the stress generated during the reaction between Si and Li is transferred to the TiNi SMA thin film. In other words, the Si thin film grown at low temperature does not have good adhesion to the TiNi SMA thin film, so it cannot transfer the stress

caused by volume changes during the charging and discharging processes. However, the Si(HT)/TiNi/Cu electrode exhibited good stress transmission to the TiNi SMA thin film owing to enhanced adhesion between the Si and TiNi thin films. It was confirmed that the Si thin film must be deposited at high temperature to obtain the stress absorption effect of the TiNi SMA thin film. More detailed investigations of the stress absorption effect of the TiNi SMA thin film need to be conducted in the future.

4. Conclusion

Si thin films were fabricated on a TiNi SMA thin film by DC magnetron sputtering at different temperatures. The structural and electrochemical properties of the Si(LT)/TiNi/Cu electrode were compared with those of the Si(HT)/TiNi/Cu electrode. The Si thin films formed were amorphous regardless of the deposition temperature. The Si(HT)/TiNi/Cu electrode exhibited excellent capacity retention until approximately the 45th cycle, whereas rapid capacity fading occurred in the Si(LT)/TiNi/Cu electrode at the same current density of 200 $\mu A/cm^2$. The improvement in the cycle performance of the Si(HT)/TiNi/Cu electrode was attributed to better adhesion between the Si thin film and the TiNi SMA thin film, resulting in transfer of the stress absorption effect to the TiNi SMA thin film.

Acknowledgement

Author Contributions

Conceptualization, J. H. Bae and J. P. Noh; Methodology, J. H. Bae; Validation, J. H. Bae and J. P. Noh; Formal Analysis, N. Oyunbayar; Investigation, J. H. Bae and D. H. Seo; Data Curation, J. H. Yang and T. H. Nam; Writing—Original Draft Preparation, J. P. Noh; Writing—Review & Editing, J. P. Noh and H. M. Jeong; Visualization, J. H. Bae and D. H. Seo; Supervision, J. P. Noh; Project Administration, S. C. Huh; Funding Acquisition, J. P. Noh.

References

[1] Y. P. Wu, E. Rahm, and R. Holze, "Carbon anode materials for Li ion batteries," Journal of Power Sources, vol. 114, no. 2, pp. 228-236, 2003.

[2] J. O. Besenhar, J. Yang, and M. Winter, "Will advanced lithium-alloy anodes have a chance in lithium-ion batteries?," Journal of Power Sources, vol. 68, no. 1, pp. 87-90, 1997.

[3] C. H. Doh, M. W. Oh, and B. C. Han, "Lithium alloying potentials of silicon as anode of lithium secondary batteries," Asian Journal of Chemistry, vol. 25, no. 10, pp. 5739-5743, 2013.

[4] M. N. Obrovac and L. Christensen, "Structural changes in silicon anodes during Li insertion/extraction," Electrochemical and Solid-State Letters, vol. 7, no. 5, pp. A93-A96, 2004.

[5] M. N. Obrovac and L. J. Krause, "Reversible cycling of crystalline silicon powder," Journal of the Electrochemical Society, vol. 154, no. 2, pp. A103-A108, 2006.

[6] J. Li and J. R. Dahn, "An In Situ X-Ray diffraction study of the reaction of Li with crystalline Si," Journal of the Electrochemical Society, vol. 154, no. 3, pp. A156-A161, 2007.

[7] C. Yu, X. Li, T. Ma, J. Rong, R. Zhang, J. Shaffer, Y. An, Q. Liu, B. Wei, and H. Jiang, "Silicon thin films as anodes for high-performance lithium-ion batteries with effective stress relaxation," Advanced Energy Materials, vol. 2, no. 1, pp. 68-73, 2012.

[8] B. A. Boukamp, G. C. Lesh, and R. A. Huggins, "All-solid lithium electrodes with mixed-conductor matrix," Journal of the Electrochemical Society, vol. 128, no. 4, pp. 725-729, 1981.

[9] M. H. Park, M. G. Kim, J. B. Joo, K. T. Kim, J. Y. Kim, H. Ahn, Y. Cui, and J. P. Cho, "Silicon nanotube battery anodes," Nano letters, vol. 9, pp. 3844-3847, 2009.

[10] Li-Feng Cui, Yuan Yang, Ching-Mei Hsu, and Yi Cui, "Carbon−Silicon Core−Shell Nanowires as High Capacity Electrode for Lithium Ion Batteries," Nano Letters, vol. 9, no. 11, pp. 3370-3374, 2009.

[11] S. Yin et al., "Silicon lithium-ion battery anode with enhanced performance: Multiple effects of silver nanoparticles," Journal of Materials Science & Technology, vol. 34, no. 10, pp. 1902-1911, 2018.

[12] G. B. Cho, B. M. Kim, and J. P. Noh et al., "Electrochemical properties of Si film electrodes with TiNi shape memory alloy as a current collector," Journal of Alloys and Compounds, vol. 577, pp. S190-S194, 2013.

[13] Y. M. Im, J. P. Noh, and G. B. Cho et al., "Electrochemical properties of Si film electrodes containing TiNi thin-film current collectors," Shape Memory and Superelasticity, vol. 4, pp. 121-126, 2018.

[14] J. Haider, M. Rahman, B. Corcoran, and M. S. J. Hashmi, "Simulation of thermal stress in magnetron sputtered thin coating by finite element analysis," Journal of Materials Processing Technology, vol. 168, no. 1, pp. 36-41, 2005.

[15] Y. Wang, S. Nakamura, M. Ue, and P. B. Balbuena, "Theoretical studies to understand surface chemistry on carbon anodes for lithium-ion batteries reduction mechanisms of ethylene carbonate," Journal of the American Chemical Society, vol. 123, no. 47, pp. 11708–11718, 2001.

[16] A. Naji, Jaâfar Ghanbaja, Bernard Humbert, Patrick Willmann, and Denis Billaud, "Electroreduction of graphite in $LiClO_4$-ethylene carbonate electrolyte. Characterization of the passivating layer by transmission electron microscopy and Fourier-transform infrared spectroscopy," Journal of Power Sources, vol. 63, no. 1, pp. 33–39, 1996.

[17] P. Novák, F. Joho, R. Imhof, J-C. Panitz, and O. Haas, "In situ investigation of the interaction between graphite and electrolyte solutions," Journal of Power Sources, vol. 81-82, pp. 212–216, 1999.